the focused beam diameter is thus reduced to 1 mm, and illumination and reflection occur at the specular angle over a solid angle that closely approaches π steradians. Thus, our bidirectional reflectance measurements actually record biconical reflectance over a large solid angle.

An aluminum mirror was used as the background reference against which sample biconical reflectance was ratioed. A mirror was used as the reference instead of Halon, because the latter exhibits strong absorption bands in most of the spectral range measured here. Not only does the mirror provide a spectrally flat reference, but its high reflectance is required when measuring the reflectance of solid samples at the wavelengths of the fundamental molecular vibration bands. As described below, minerals have a mirrorlike opacity at such wavelengths, and smooth solid samples may have reflectances close to that of a mirror. Use of biconical reflectance with a mirror reference makes the measured reflectance of a diffusely reflecting particulate sample roughly a factor of five lower than it would be for the integrating sphere measurements commonly made in the visible and near-infrared.

The Nicolet 5DXB and System 510 can switch the infrared beam from the sample compartment to an external port, through which it exits in collimated form. An integrating sphere, coated inside with a diffusely reflecting gold surface, was attached to the instrument at this port. The sphere is 12.7 cm in diameter and has a 2.5 cm diameter entrance port in the top of the sphere at 10° off the vertical, through which the beam passes to fall on a 2.5 cm diameter sample/reference port in the bottom of the sphere. Beam size on the sample in that bottom port is 1.54 cm. A 2.5 cm detector port is placed at an angle of 90° to the principal plane in the side of the sphere, and the liquid-nitrogen-cooled MCT detector chip is baffled to eliminate direct viewing of either the sample or the specular "hot spot" on the sphere wall. A port at the specular angle was filled during the measurements reported below with a gold-coated plug having a surface curved to match the interior curvature of the sphere.

The integrating sphere uses a Labsphere diffuse gold surface as a reference. Sphere performance was carefully calibrated to provide absolute reflectance by comparing measured reflectances of Halon, a front-surface aluminum mirror, water, and a black body cone with values obtained from the National Bureau of Standards or found in the literature (Salisbury and Milton, 1987).

The usual sample holder for biconical reflectance measurements was 13 mm in diameter and 2 mm deep, although a "microreflectance" holder 3 mm x 2 mm could also be used for very small samples. The usual sample holder for hemispherical reflectance measurements was 2.5 cm in diameter and 3 mm deep. That samples were optically thick at a depth of 2 mm was verified by comparison of spectra measured in bare aluminum cups with spectra measured in cups painted black. Most particulate samples were sifted into the sample holders to attempt to achieve random orientation of grains. For some samples, including all of the clay minerals, solid samples were not available. In these cases, the fine powder samples were packed into a pseudo-solid sample so that the reflectance peaks of the fundamental molecular vibration (reststrahlen) bands could be seen. This was accomplished with <2 μm clays by placing them in a folded weighing paper and gently rolling a sample bottle over the outside surface. This produced cohesive flakes that could be readily transferred to the reflectance attachment and measured. Some samples, such as the olivines, were not sufficiently fine-grained to produce flakes. To make packed sample measurements of these samples, they were simply pressed into a sample cup with the flat side of a spatula. Solid samples were fixed in a bed of moldable erasure to hold the surface being measured in a horizontal position. All samples could be raised or lowered by a micrometer screw mechanism so that the measurement surface was at the beam focus.

The Nicolet scans an interferogram each second. Interferograms are then averaged to provide the desired signal-to-noise after deconvolution to a spectrum. This normally required 100 scans for transmittance measurements and 500 to 1000 scans for reflectance.

Major Spectral Features of Minerals

The spectral features of minerals in the wavelength range considered here are the result of vibrational processes. Their number, intensity and shape are dependent on atomic masses, interatomic force fields and, particularly, molecular geometry. One goal of the spectroscopist is to quantitatively describe the vibrational process so that the origin of each absorption band can be understood. Sophisticated calculations have been made that are consistent with observation, at least for the simpler minerals (e.g., Elcombe, 1967), although not necessarily correct or final. Even if a vibrational mode were understood precisely, it is virtually impossible to describe such a motion simply and concisely for such complex structures as silicates. Consequently, one must rely on some very general description, such as "Si-O symmetric stretch," to describe all those vibrations which predominantly involve the symmetric expansion and contraction of the silicon-oxygen bonds. Using such simplified visualizations, we can successfully generalize about the spectral behavior of minerals. For example, lighter atoms vibrate at higher frequencies (shorter wavelengths) than heavier atoms when substituted into the same structure (see olivines, p. 168–192). Higher bond strengths also result in higher frequencies of vibration, and this change in bonding in silicates is related to the degree of polymerization of the $Si\text{-}O_4$ ion (Walter and Salisbury, 1989). This results in a systematic change in wavelengths of the fundamental vibration bands of silicates as the framework structure ultimately gives way to isolated tetrahedra. Finally, bond-stretching vibrations in covalent structures lie at higher frequencies than bending modes, and such internal molecular vibrations typically lie at higher frequencies than lattice modes (Farmer, 1974).

The most prominent features in the infrared spectra of minerals can be understood in the context of the generalizations outlined above and are described below for different types of minerals. In particular, we point out those bands seen in reflectance or emittance that are not apparent in the trans-

mittance spectra typically studied by others. This discussion of the origins of spectral features is not repeated in the text for each mineral, because it would prove highly repetitious for the relatively well understood bands, such as the fundamental internal molecular vibration bands of the minerals and associated water and hydroxyl. Those bands can easily be identified in the spectra of each mineral on the basis of the discussion below. The attribution of more complex features due to overtones and combination tones of the internal vibrations and lattice modes is a more speculative matter, even for the simplest of minerals. Such speculation would also be repetitious and is not the function of this work. Farmer (1974) discusses the spectral features of minerals at length, and Farmer and Palmieri (1975) provide an exhaustive list of references categorized by mineral. Estep-Barnes (1977) presented a good review of the major spectral features of minerals, accompanied by an extensive bibliography. The interested reader is referred to these works for the best information on the subject of detailed band assignments.

Silicates

The most intense spectral features of silicates, occurring between 8 and 12 μm, are generally described as due simply to fundamental asymmetric Si-O-Si stretching vibrations, but Si-O-Al stretching vibrations may also contribute when aluminum is part of the crystal lattice (for the classic Si-O-Si stretching feature, see the 9.2 μm band in quartz in Figure 1A). The appearance of these features typically changes in reflectance because of the role of the refractive index in scattering (see "The Role of Surface and Volume Scattering," below). The weak side band near 8.5 μm in the transmittance spectrum of quartz, for example, becomes a well-defined lobe of a prominent reflectance doublet between 8 and 10 μm in Figure 1B. The reflectance spectrum of a quartz glass displays a much weaker short-wavelength lobe (Figure 1E), which in some cases of shocked quartz we have seen is reduced to a shoulder. This simplification of glass spectra of minerals is well known and is attributed generally to broadening of the bands (e.g., Farmer, 1974, p. 484). However, broadening would not appear to explain the reduced intensity of the 8.5μm band in the spectrum of glass compared to that of crystalline quartz. An alternative explanation is that the short-wavelength lobe of the strong quartz reflectance doublet is not due entirely to internal molecular vibrations but depends to some extent on long-range order (Simon and McMahon, 1953). Whatever the details of their origin, these most intense features fall in the 8–14 μm atmospheric window, making them the most useful for terrestrial remote sensing of silicates (Kahle and Goetz, 1983; Walter and Salisbury, 1989).

The second most intense silicate bands are broadly characterized as O-Si-O deformation or bending modes, which occur in the 18–25 μm region. Again, aluminum and, indeed, other cations may contribute additional band structure in this region (Farmer, 1974, p. 365). The relative intensities of the two quartz bands in this spectral region appear unchanged in reflectance compared to transmittance (compare Figures 1B and 1C) but have been shifted about 1 μm to shorter wavelength by the interaction of absorption coefficient and refractive index on the scattered light, which is typical (Salisbury et al., 1987b). The weaker feature occurring at 18.3 μm in reflectance completely disappears in the spectrum of fused silica in Figure 1E, indicating such a strong dependence on long-range order that it must be due to a lattice vibration.

Weaker bands in quartz spectra between 12 and 15 μm have been attributed to symmetric Si-O-Si stretching vibrations (Farmer, 1974, p. 366). When some of the silicon atoms are replaced by aluminum, as in the feldspars, additional Si-O-Al stretching vibrations are added over a longer wavelength range. For example, albite displays eight highly characteristic bans in its spectrum between 12 and 20 μm (see p. 12). Again such bands are greatly simplified or eliminated in the spectra of glasses (Figure 1E; see also Nash and Salisbury, 1991).

Figures 1C and 1D show additional weak bands displayed as troughs between 3 and 7 μm. Such bands in silicate spectra have been largely ignored because they are usually too weak to be seen in transmittance spectra (compare Figure 1A). However, they can be very useful in the spectral identification of fine particulate minerals and rocks, where they are quite prominent (Salisbury et al., 1987b; Salisbury and Walter, 1989; and Salisbury et al., 1991). Because they have not been assigned with any certainty, we refer to such bands simply as overtone/combination tone bands of internal and lattice modes.

Carbonates

The strongest bands of carbonates are due primarily to fundamental internal molecular vibration bands of the CO_3 ion, which are well understood (Farmer, 1974, p. 231). Carbonates typically display a strong band near 7 μm due to asymmetric C-O stretching vibrations and weaker bands near 11.4 and 14.3 μm due to bending modes, which can be seen in the spectrum of calcite (p. 54). Very weak bands in the transmittance spectrum to shorter wavelength than 7 μm are strongly displayed as troughs in the reflectance spectrum of particulate calcite. Because of their relative visibility in transmittance spectra, these weak bands have been the subject of study and appear to be due to combination tones of internal and lattice modes (Farmer, 1974, p. 236).

Sulfates

The sulfate ion displays a group of intense stretching fundamentals near 8.7 μm and two or more bending modes near 16 μm, as can be seen in spectra of gypsum (p. 102) and anhydrite (p. 30). Again, the weaker features in transmittance spectra of sulfates at shorter wavelength than the strong stretching fundamental are strongly displayed in reflectance spectra of particulate samples. The complex feature near 4.6 μm appears to be a combination tone of the sulphate ion, perhaps accompanied by water combination tones (Hass and Sutherland, 1956). The features near 2.8 and 6.2 μm are due to water, the spectral features of which are discussed separately below.

Oxides

The metal-oxygen stretching vibration bands in oxides occur at longer wavelength than the Si-O features (see, e.g., chromite, p. 62). An interesting aspect of these features is that, because of the intense dipole oscillations induced by the vibrations of highly ionic oxides, their powder spectra are profoundly modified by the shape and size of the particles (Farmer, 1974, p. 183). Thus, it is sometimes uncertain whether variations in powder spectra given by different specimens of a given compound are due to real differences in purity or phase, or merely to shape and size. A case in point is provided by spectra of our two goethite samples (see p. 96 and 98).

Sulfides

Most metal-sulphur vibration bands lie beyond our wavelength range in the far-infrared. We have included two examples (pyrite, p. 204, and pyrrhotite, p. 210) that do show bands within our wavelength range.

Water and Hydroxyl

The most common vibration bands in minerals are due to water and hydroxyl, the spectral features of which have been thoroughly reviewed by Aines and Rossman (1984). When water is not fixed in a crystal lattice but is hydrogen-bonded to other water molecules, it results in a broad spectral feature centered near 2.9 μm due to O-H stretching vibrations and another near 6.1 μm due to H-O-H bending vibrations (see Figure 1A). Such water may be present in fluid inclusions, as interlayer water in sheet silicates, or as water of hydration. Water in a crystalline environment produces sharper O-H stretching absorption features than occur in the liquid water spectrum, which typically also occur at a shorter wavelength. Multiple O-H stretching vibrations can result when water is present at several sites in the crystal lattice. Beryl (p. 44) and cordierite (p. 74), for example, contain water that resides at specific sites in channels parallel to the C axis (Aines and Rossman, 1984). These minerals are also interesting because they typically have CO_2 trapped in these channels, which produces sharp bands near 4.3 μm (compare atmospheric CO_2 bands in Figure 2 with spectra of beryl and cordierite).

Minerals containing hydroxyl without water display O-H stretching features near 2.7 μm but lack the broad feature at 2.9 μm and the H-O-H bending mode at longer wavelength. A good example is kaolinite (p. 132), which has no interlayer water. Most often, however, minerals display a combination of hydroxyl and molecular water bands, as in the case of antigorite (p. 34).

Many minerals contain a trace of OH and water, although this is not reflected in their chemical formulae. A good example is quartz, which typically displays multiple sharp O-H stretching features superimposed on a weak broad water band (see Figures 1C and 1D). The broad water band is probably due to a small amount of liquid water in fluid inclusions. The sharper hydroxyl features are associated with hydroxylated alkali metals that serve to balance charges when aluminum substitutes for silicon (Aines and Rossman, 1984).

In addition to the fundamental O-H and H-O-H features commonly seen in the spectra of minerals in the 2–7 μm region, a variety of significant metal cation-OH bands can be found at longer wavelength, especially in clay minerals (Stubican and Roy, 1964). Kaolinite, for example, displays a prominent Al-OH band near 11 μm (see p. 132).

OH lattice vibrations are typically seen at still longer wavelengths (Farmer, 1974, p. 348), such as the 16 μm feature in the spectrum of antigorite (see p. 34).

Water and hydroxyl bands are spectrally important because most silicate minerals capable of doing so have undergone incipient alteration to hydrous phases and/or contain fluid inclusions, even when appearing quite fresh, because of the ubiquity of water in the terrestrial environment. This is in marked contrast to other environments, such as that of the moon (Roedder, 1984). It should be pointed out that water and hydroxyl are usually not present in large amounts where they are not part of the mineral stoichiometry. However, spectral features due to water and hydroxyl may be very prominent, especially in reflectance spectra of fine particulate materials. This is due to the enhancement of such absorption bands by the increased scattering associated with fine particle size, which is discussed below. Thus, an estimate of the abundance of water and hydroxyl relative to other phases can best be obtained from transmittance spectra.

Discussion of Spectra

Role of Surface and Volume Scattering

All major studies of the nature of mineral spectra have used transmittance data (Farmer, 1974; Farmer and Palmieri, 1975, and references therein). Transmittance spectra are simpler to interpret than reflectance or emittance spectra, because they depend solely on the absorption coefficient. Reflectance and emittance spectra involve both the absorption coefficient and the refractive index, which causes spectral features to change quite significantly, especially when scattering becomes important in particulate samples (Salisbury et al., 1987b).

It is apparent from inspection of our mineral spectra that particle size has a very significant effect on reflectance spectra. A mathematical model of reflectance from particulate samples has been developed by Hapke (1981). We focus here on a qualitative physical model to provide a basic understanding of how and why spectral features change with particle size, addressing the role of surface and volume scattering.

The radiation returned to the observer in reflectance from a particulate sample has been scattered by the particles. This scattering takes place by two processes: surface scattering, which involves rays that have reflected from the surfaces of grains without penetration; and volume scattering, which involves rays that have been refracted into grain interiors and then scattered or refracted back out. Which of these processes dominates returned radiation is determined primarily by the absorption coefficient and particle size (Vincent and Hunt, 1968).

The wavelength variation in absorption coefficient can be

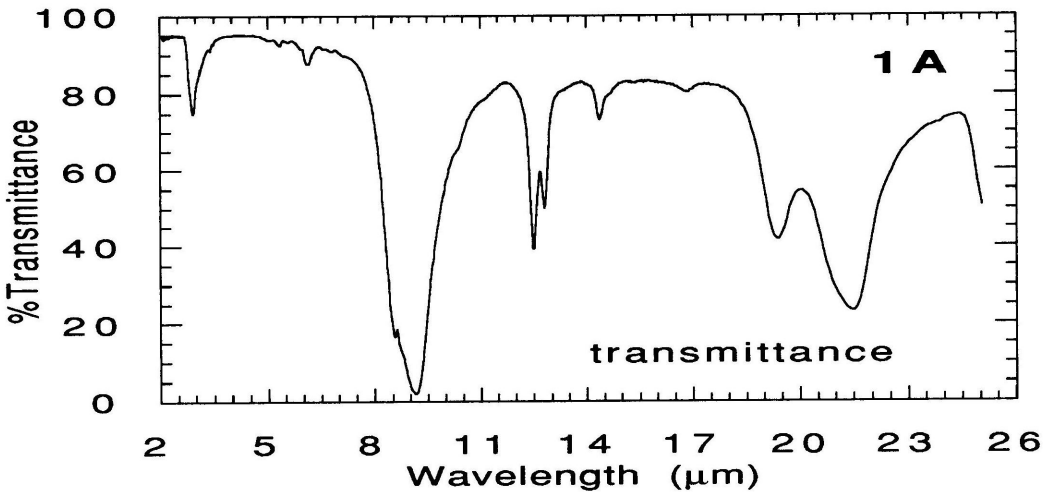
100
80
60
40
20
0
%Transmittance
1A
transmittance
2 5 8 11 14 17 20 23 26
Wavelength (μm)

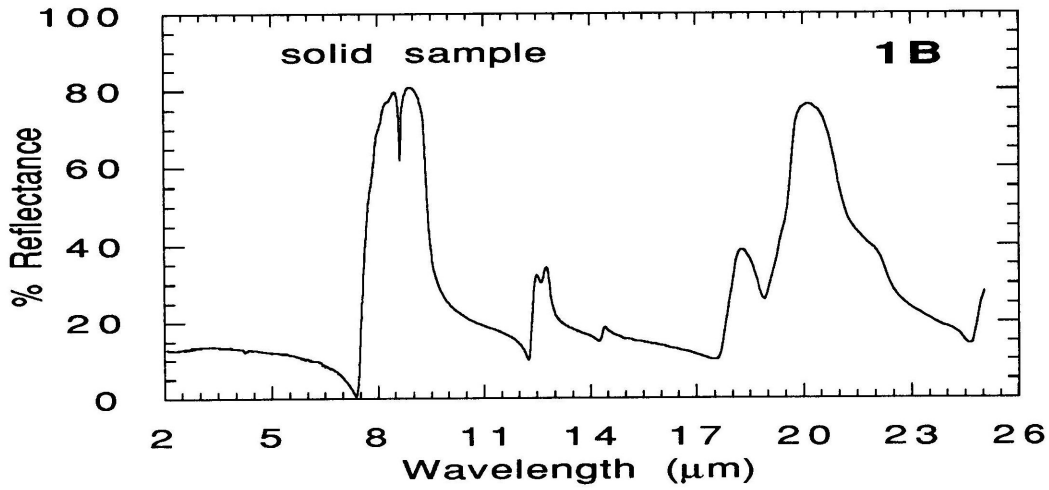
100
80
60
40
20
0
% Reflectance
solid sample
1B
2 5 8 11 14 17 20 23 26
Wavelength (μm)

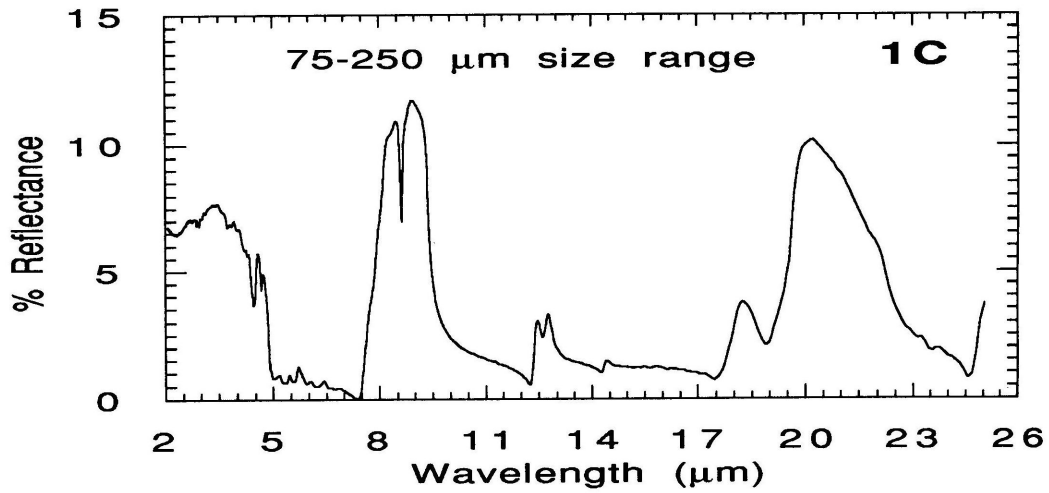
15
10
5
0
% Reflectance
75-250 μm size range
1C
2 5 8 11 14 17 20 23 26
Wavelength (μm)

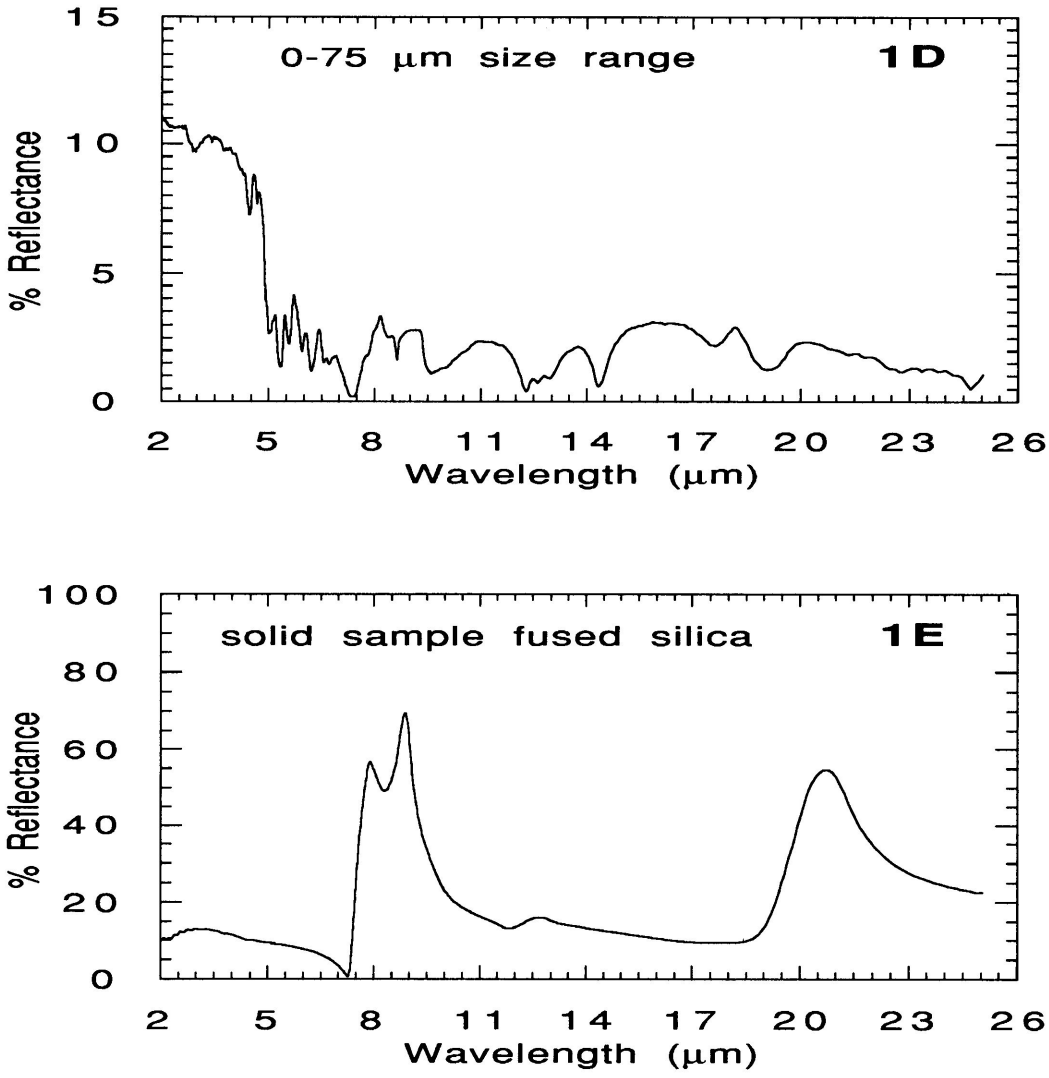

Figure 1. Spectra of quartz in transmittance (A), and in reflectance for a solid sample (B), 75–250 μm size rance (C), and 0–75 μm size range (D). Spectral reflectance of high purity fused silica produced by Corning Glass is shown for comparison (E).

determined from a transmittance spectrum. This can be illustrated in Figure 1A, where the highest absorption coefficient for the mineral quartz is associated with the Si-O stretching vibration near 9.2 μm. A weaker band due to the bending mode near 21.5 μm is accompanied by the still weaker feature near 19.5 μm, and progressively weaker stretching features can be seen near 12.5, 12.7 and 14.5 μm.

The transmittance spectrum in Figure 1A shows, then, spectral features with a wide range of absorption coefficient; and Figures 1B, 1C, and 1D illustrate the effects of particle size on those spectral features in reflectance.

Figure 1B shows reflectance from the smooth surface of a solid sample which, of course, eliminates multiple scattering. As a result, the entire spectrum is dominated by simple Fresnel reflectance from the surface (Salisbury et al., 1987b), and the spectral features are reflectance peaks associated with the strongest molecular vibration bands. The correlation of reflectance *peaks* with very strong *absorption bands* is counterintuitive to those researchers accustomed to working in the visible and near-infrared. This effect is due to the very strong absorption coefficient associated with these bands, which induces a mirror-like opacity at these wavelengths.

Comparison of Figures 1B and 1C shows the effect on spectral reflectance of changing from a single slab surface to a 75–250 μm particle-size range. The reflectance peaks, or "reststrahlen bands," discussed above are still apparent between 7.5 and 24 μm. However the appearance of the spectrum between 2.1 and 7.5 μm has changed significantly. Weak but distinct alkali metal-OH features can be seen between 2.8 and 3.2 μm, and a series of overtone/combination tone bands are visible between 3.5 and 7.5 μm. These spectral features are all expressed as troughs, not peaks, showing that this region of the spectrum is dominated by volume scattering. What has occurred is that the particle size has become small enough, on average, to allow passage of photons completely through the grains in this spectral region of relatively low absorption coefficient. That is, the grains are optically thin. More photons are absorbed in band centers than in band wings during volume scattering, and reflectance minima (troughs) occur.

Thus, for particulate silicates, the spectral range documented in this library is generally dominated by volume scattering and absorption band troughs on the left side of each figure and by surface scattering and absorption band peaks on the right side. The dividing line is the sharp minimum in reflectance associated with the principal Christiansen frequency (see below) displayed in Figure 1 at 7.4 μm.

Changes in Spectral Contrast

Considering first the reflectance minima associated with volume scattering, band depth (Clark and Roush, 1984) is a measure of band intensity commonly referred to as spectral contrast. It is apparent in Figure 1C and 1D that this spectral contrast changes with changing particle size. However, the change is not consistent, spectral contrast sometimes increasing and sometimes decreasing with decreasing particle size. The explanation for this behavior lies in the relationship between mean optical path length and particle size, which can be illustrated with three cases. Mean optical path length (MOPL) is the mean distance photons will pass through a material before total absorption takes place (Clark and Roush, 1984). When the absorption coefficient is relatively high and the MOPL is much less than the mean grain diameter in a particulate sample, all photons entering the grains are absorbed. If the MOPL remains smaller than the mean particle diameter, even at a finer particle-size range, photon absorption remains essentially unchanged. Something close to this first case is seen in the centers of the overtone/combination tone bands near 5.4 and 6.2 μm. The reflectance in these band centers increases only slightly in the spectrum of the finer particle-size range compared to that of the coarser size range (i.e., the band remains nearly saturated). A better example is seen in the center of the hydroxyl stretching fundamental near 2.7 μm in the spectra of antigorite (p. 34). The band center remains saturated at about 1% reflectance for both coarse and fine particle-size ranges.

A second case occurs at intermediate absorption coefficient when the MOPL is initially on the order of the mean grain diameter. As the particle size decreases, many more photons survive passage through the grains and a significantly larger portion of the incoming radiation will be scattered back in the direction of the observer. This second case applies to the wings of the 5.4 and 6.2 μm bands of quartz and to the wings of the hydroxyl band of antigorite.

When the reflectance in the wings of a band rise significantly with decreasing particle size (Case 2), while the band center remains saturated or nearly so (Case 1), an increase in spectral contrast occurs. This effect causes absorption bands having the right ranges of absorption coefficient between band wings and band centers to display intense bands at fine particle size. This occurs not only for many of the silicate overtone/combination tone bands (especially for quartz and olivine) but also for carbonate and sulfate combination tones and the fundamental O-H and C-H stretching vibration bands. Thus, spectra of fine particulate mineral mixtures may be dominated out of proportion to their abundance by minerals that display such spectral behavior, as shown elsewhere for igneous rocks and meteorites (Salisbury and Walter, 1989; Salisbury et al., 1991).

A third illustrative case occurs when the MOPL is already much greater than mean particle diameter at the coarser particle size. In this case, the bulk of potentially backscattered radiation is already returned to the observer at large particle size. Thus, a reduction is mean grain diameter has proportionally less effect than when MOPL starts out close to mean grain diameter. This third case applies to the wings of the weaker overtone/combination tone band near 4.5 μm. Here the wings rise relatively less than the band center. which is affected more by Case 2 scattering. Thus, this band *decreases* in spectral contrast with decreasing particle size, which is the norm for weak bands displayed in the visible and near-infrared.

We turn now to the reststrahlen bands dominated by surface scattering. These absorption bands produce prominent reflec-

tance peaks in Figures 1B and 1C, which are greatly reduced in intensity in Figure 1D. In fact, the weakest reststrahlen reflectance peak at 14.5 μm turns into a trough at the finest particle size. While changing particle size may have resulted in changes in single-particle albedo and scattering geometry (Conel, 1969), Salisbury and Eastes (1985) focused on a physical model depending on porosity to explain the decline in spectral contrast of the reststrahlen bands. They noted that when a very fine (<5 μm) powder is packed to reduce porosity, its spectrum displays reflectance peaks as prominent as those displayed by the coarser particle-size ranges. They suggested that the increased porosity associated with fine particle size resulted in formation of photon traps. That is, that the pores acted like small black bodies. A similar explanation was offered earlier by Lyon (1964) and Aronson et al. (1966). However, research in progress suggests that the change in shape and intensity of the reststrahlen bands is due more to the occurrence of substantial volume scattering at fine particle size rather than to photon trapping, which is essentially a surface scattering effect. Briefly, it appears that the role of porosity is to physically separate 1–5 μm diameter particles that are optically thin, even in the reststrahlen bands (Hunt and Logan, 1972). When such particles are separated by more than a wavelength, they scatter independently as optically thin, volume-scattering particles. When packed closely together, however, they scatter coherently as if they were large, optically thick, surface-scattering particles. Thus, the loss of spectral contrast of reststrahlen bands for materials of fine particle size appears to be due directly to particle size and only indirectly (but critically) to porosity.

It is important to note in any discussion of the spectral contrast of reststrahlen bands that such bands do persist in spectra of fine materials, even if reduced in intensity and changed in shape. In addition, the reststrahlen bands of some minerals are more persistent than those of others. As shown by Salisbury and Walter (1989) and Salisbury et al. (1991), quartz, olivine, and pyroxene display such persistent reststrahlen bands. Thus, the reststrahlen region may suffer reduced spectral contrast but is by no means either featureless or useless in spectra of particulate mineral mixtures.

Transparency Peaks

We have referred to the region of the spectrum where the reststrahlen bands occur as dominated by surface scattering. This is obviously true for solid samples of silicates and for the coarse particle-size range, which exhibit prominent reflectance peaks (Figures 1B and 1C). However, it can be seen in the transmittance spectrum of quartz (Figure 1A) that a region of relatively high transparency exists between the asymmetric and symmetric stretching vibrational features in the vicinity of 10.5 to 12 μm. The absorption coefficient here is low enough so that grains become optically thin and volume scattering of the Case 2 type (see above) occurs as the particle-size range is reduced from 75–250 μm to 0–75 μm (Figures 1C and 1D). Because the strong reststrahlen reflectance peaks are greatly diminished at fine particle size, the broad transparency peak becomes a prominent feature centered at about 11 μm. Such transparency peaks may be very prominent in the spectra of some minerals (e.g., antigorite, p. 34).

Transparency peaks were first noted without explanation in reflectance spectra of rocks by Hovis and Callahan (1966). Conel (1969) described and explained such features (expressed as troughs in emittance) in spectra of quartz. Salisbury and Walter (1989) showed that the wavelength of the transparency peak could be related to the composition of igneous rocks. Documented here is the spectral behavior of a wide range of rock-forming minerals, showing the nature and magnitude of transparency peaks that occur in reflectance of fine particulate samples.

Note that the prominence of this feature is dependent on the degree to which the adjacent reflectance peaks associated with the reststrahlen bands are diminished in spectra of the fine particle-size range. As explained above, the loss of these peaks appears to be related to the increased porosity and volume scattering in a sample due to very fine particle size. When a sample is sifted into a sample cup, the finest particles tend to be suspended in air and drift away during sifting. Thus, a sample sifted and measured repeatedly will tend to increase in mean grain diameter and to display progressively stronger reststrahlen bands. We have attempted to avoid this with our samples, but there is some obvious variability of reststrahlen-band spectral contrast (compare acmite.1, p. 8, and acmite.2, p. 10). Also, a few samples were not prepared by us and vary in particle-size range as a result (olivine.4, p. 174, for example, is completely lacking in very fine particles).

Despite the fact that some minerals fail to display transparency features, it is apparent from the spectra in this volume that such peaks (expressed as troughs in emittance) could be prominent spectral features in the 8–14 μm spectrum of a fine-particulate regolith. Salisbury et al. (1991) suggest that the distortion of a spectrum by the sharp thermal gradient associated with a vacuum environment may make such broad features difficult to detect, but further measurements of appropriate candidate materials in a simulated space environment are needed to confirm this.

Christiansen Feature

A final spectral feature that is prominent at fine particle size is associated with the principal Christiansen frequency. This is a reflectance minimum that occurs because the real part of the refractive index undergoes rapid changes (anomalous dispersion) at a slightly shorter wavelength than the most intense molecular vibration band. Consequently, the refractive index approaches 1, resulting in a minimum of scattering, at a wavelength where absorption is still relatively low. With little scattering and little absorption, infrared radiation can penetrate a sample relatively easily, resulting in a minimum in reflectance or a maximum in emittance. This feature can be seen in reflectance at all particle-size ranges, but it is one of the more easily recognized spectral features in reflectance of the finest particle-size range, as can be seen in Figure 1D at 7.3 μm. Conel (1969) first showed that the wavelength of this feature is a good indicator of mineralogy. Logan et al. (1973)

showed that the wavelength of this feature can also be used to determine igneous rock type and demonstrated its utility for mapping compositional variations in the lunar regolith. The relationship between wavelength of the Christiansen feature and composition has been determined on a more quantitative basis for igneous rocks by Salisbury and Walter (1989) and for meteorites by Salisbury et al. (1991).

Effect of Crystallographic Orientation

Many minerals are birefringent and have a different spectral response depending on crystallographic orientation. This is illustrated in the solid sample spectra of orthoclase (p. 194). The occurrence of such orientation effects is what makes it necessary to sift particulate samples, or at least their upper millimeter, into sample cups for measurement. Tapping a cup or using a knife edge to level a sample tends to orient the grains, especially if the mineral has a prominent cleavage. Some samples having an extremely asymmetric shape, such as micas, will tend to develop grain orientation despite sifting. Our laboratory studies of calcite show, however, that more equant grains are randomly oriented when sifted, despite very strongly developed cleavage.

Effect of Packing

As discussed above in the section on spectral contrast, it has been shown that packing a fine particulate sample to reduce its porosity will greatly increase the prominence of the fundamental molecular vibration bands. Thus, spectra of packed samples are presented for some minerals, such as clays, for which coarse-grained samples showing the fundamental molecular vibration bands are not available. Packing will tend to orient the grains parallel to their strongest cleavage or parting, so that these spectra are most similar to solid sample spectra obtained in that orientation. This can be illustrated with olivine.11 (p. 188), which is a magnesian olivine with a weak cleavage. Thus, the spectrum of the packed 0–75 μm sample is much closer to that of the solid-sample spectrum than it is to that of the randomly oriented 75–250 μm size range.

Effect of Atmospheric Gases

A spectrometer must be vigorously purged with dry nitrogen (or dry air from which CO_2 has been removed) in order to avoid incorporating band structure due to atmospheric H_2O CO_2 (see Figure 2) in the spectra. Spectra of same samples were obtained without adequate purging and display extremely weak atmospheric bands (compare Figure 2 and the solid-sample spectrum of acmite.1, p. 9). These atmospheric bands are usually easy to identify and do not interfere with the major molecular vibration bands of the silicates, so these spectra were retained in the library. The digital data from which Figure 2 was derived are included on the CD-ROM (subdirectory: FIGURES; file name: ATMOS.BDS) for comparison with mineral spectra where questions of atmospheric contamination may arise, or for identification of CO_2 gas inclusions in such minerals as beryl, cordierite, and topaz.

Effect of Impurities

Two kinds of impurities introduce spectral artifacts: those that are added to the sample during laboratory processing and those that were an original part of the sample. Impurities added include water (in KBr pellets) and hydrocarbon, while the most common impurities within samples are quartz, calcite, and products of exsolution and alteration.

KBr pellets are pressed under vacuum to remove water, but the material is so hygroscopic that this process quickly begins to reverse. The method chosen to compensate for this was to ratio the sample pellet transmittance against that of a blank pellet made under identical circumstances. If the KBr for both pellets was initially ground to the same particle size so that the same surface area was available to atmospheric water vapor, held under vacuum for the same amount of time

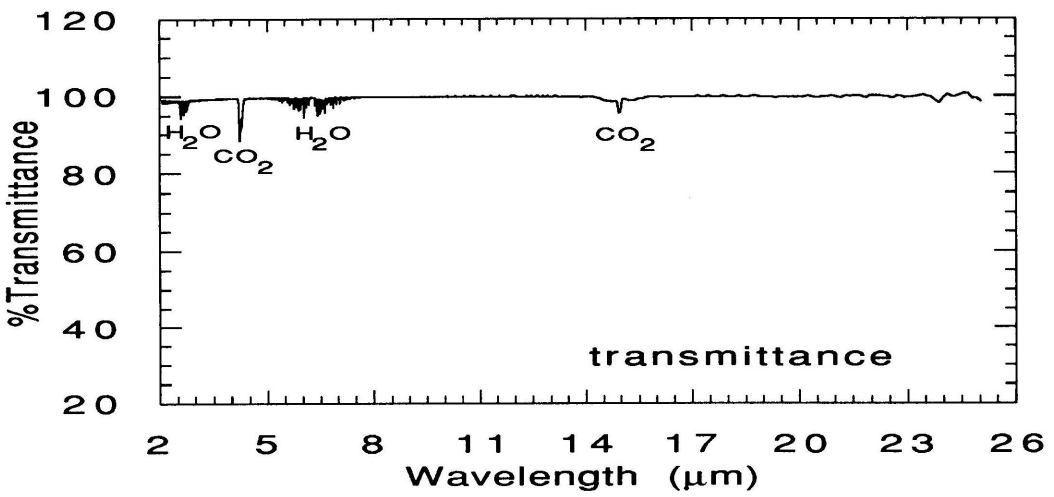

Figure 2. Atmospheric transmission spectrum showing band structure due to water vapor and carbon dioxide.

Mineral: Gypsum (alabaster) $CaSO_4 \cdot 2H_20$

File Name: Gypsum.1

Locality: Pomaia, Italy.

Source: Hunt and Salisbury Collection #26B (purchased from Ward's Natural Science Establishment).

Petrographic Description: The sample was white, translucent, and appeared pure, both in hand sample and under the microscope.

XRD Analysis: Pure gypsum.

Chemistry: None.

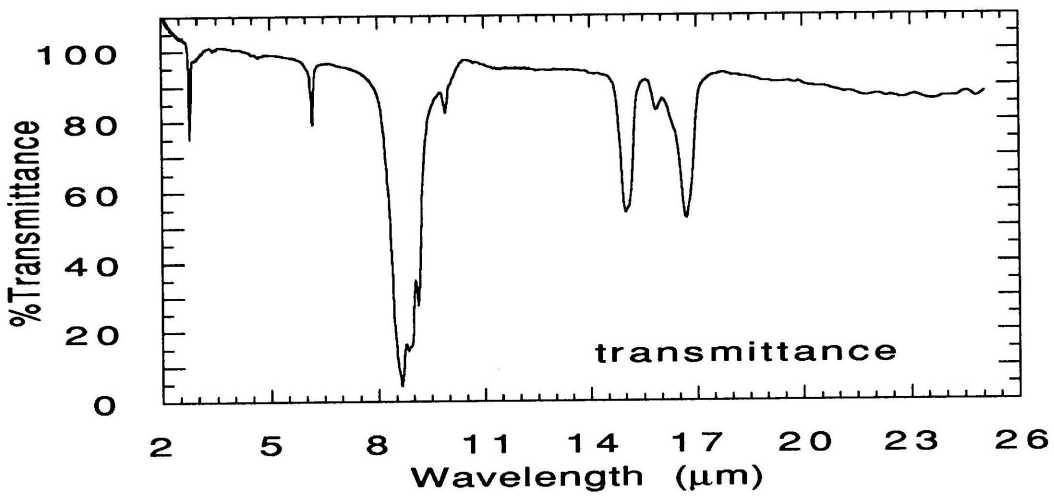

gypsum.1

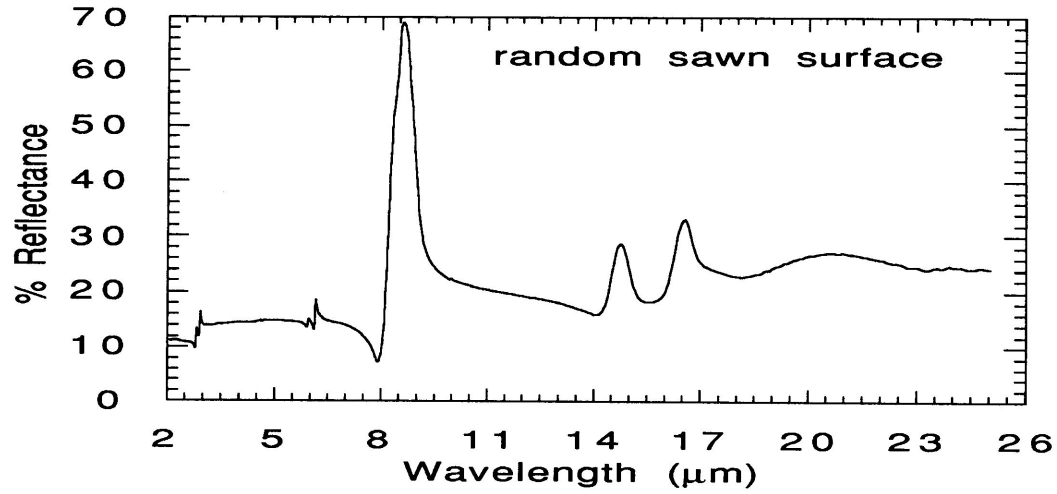
random sawn surface
% Reflectance
0
10
20
30
40
50
60
70
2
5
8
11
14
17
20
23
26
Wavelength (μm)

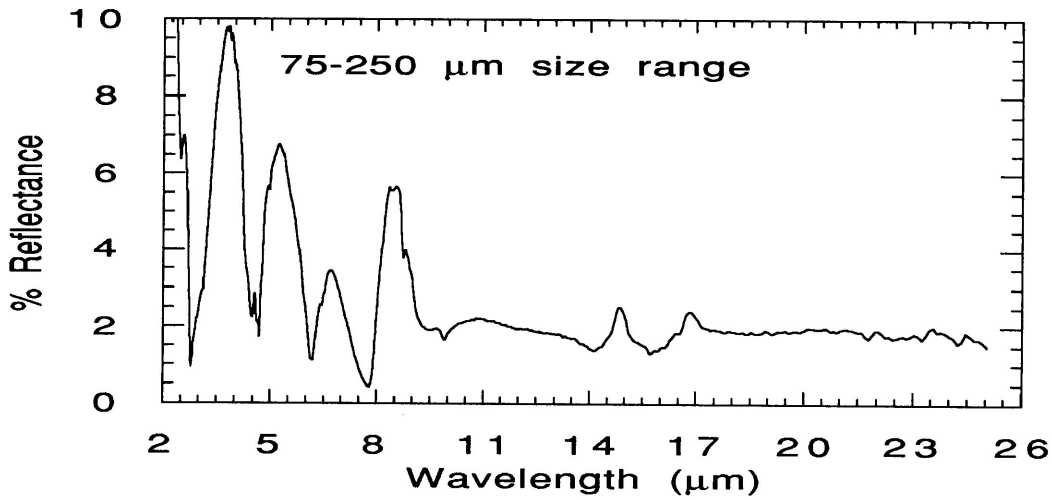
75-250 μm size range
% Reflectance
0
2
4
6
8
10
2
5
8
11
14
17
20
23
26
Wavelength (μm)

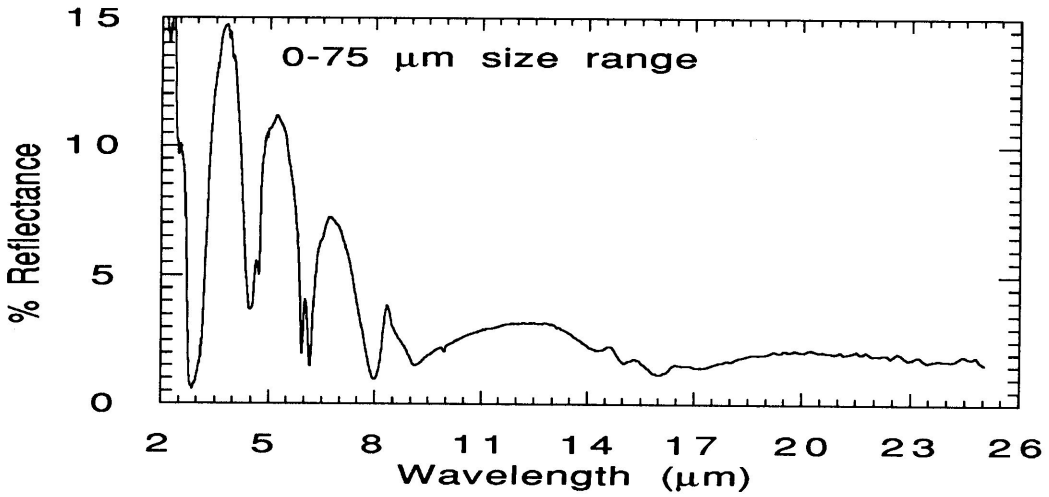
0-75 μm size range
% Reflectance
0
5
10
15
2
5
8
11
14
17
20
23
26
Wavelength (μm)